Electric field controlled nanoscale contactless deposition using a nanofluidic scanning probe

Joël Geerlings,[1,a)] Edin Sarajlic,[2] Erwin J. W. Berenschot,[1] Remco G. P. Sanders,[3] Martin H. Siekman,[4] Leon Abelmann,[3,5] and Niels R. Tas[1]
[1]*Mesoscale Chemical Systems, MESA+ Institute for Nanotechnology, University of Twente, P.O. Box 217, 7500 AE Enschede, The Netherlands*
[2]*SmartTip B.V., P.O. Box 347, 7500 AH Enschede, The Netherlands*
[3]*Transducers Science and Technology, MESA+ Institute for Nanotechnology, University of Twente, P.O. Box 217, 7500 AE Enschede, The Netherlands*
[4]*Physics of Interfaces and Nanomaterials, MESA+ Institute for Nanotechnology, University of Twente, P.O. Box 217, 7500 AE Enschede, The Netherlands*
[5]*Korea Institute of Science and Technology - Europe, Campus E7 1, 66123 Saarbrücken, Germany*

(Received 20 March 2015; accepted 28 August 2015; published online 23 September 2015)

A technique for contactless liquid deposition on the nanoscale assisted by an electric field is presented. By the application of a voltage between the liquid inside a (FluidFM) nanofountain pen AFM probe and a substrate, accurate contactless deposition is achieved. This technique allows for the deposition of polar liquids on non-wetting substrates. Sodium sulfate dried deposits indicate that the spot size and height increases with $t^{0.33\pm0.04}$ and $t^{0.35\pm0.10}$, respectively. The minimum observed diameter was 70 nm. By measuring the probe deflection and the electric deposition current, we confirm that deposition is truly non-contact. We propose a simple model based on a constant stream of liquid to the substrate, which explains our observations qualitatively. © *2015 Author(s). All article content, except where otherwise noted, is licensed under a Creative Commons Attribution 3.0 Unported License*. [http://dx.doi.org/10.1063/1.4931354]

The electrically assisted deposition of aqueous droplets is a promising technique for the deposition of polar and ionic components, which after the evaporation of the solvent will form solids. This opens applications in the field of nanolithography and 3D nanofabrication. Furthermore, the use of water as the main solvent in this process allows the deposition of biomolecules. It is known that biomolecules will stay predominantly intact during electrospraying.[1]

Liquid deposition on surfaces by means of AFM techniques was introduced by Piner *et al.*[2] This technique was termed dip-pen nanolithography (DPN) and allows for the deposition of structures as small as 15 nm. The shortcoming of the necessity to regularly recoat and realign the tip during the patterning can be overcome by direct integration of a liquid reservoir into the probe. This method was introduced by Meister *et al.*[3] and is termed nanoscale dispensing (NADIS). While the deposition by DPN is dominated by dissolution kinetics and the diffusive transfer of molecules,[4,5] NADIS relies on liquid spreading, thereby allowing the deposition of larger particles (for example, nanoparticles or proteins).[6] Both DPN and NADIS are dependent on the tip-liquid-substrate interaction, which makes the use of aqueous solvents difficult.

In this letter, we extend the NADIS work by presenting electrically assisted deposition, thereby introducing electrowetting and electrokinetic flow into the deposition process. This method allows for the deposition of liquids on non-wetting surfaces, which is challenging for deposition techniques that rely primarily on liquid spreading (whether by capillarity or pressure driven). We made use of closed fluidic AFM probes termed nanofountain pen probes[7] (further developed under the name FluidFM).[8] We demonstrate that the precise z-control of the probes in AFM leads to smaller features sizes than can be obtained by e-jet using capillaries.[9] Significant z-deflection can be expected due to the electrostatic attraction on the probe; therefore, we incorporated a z-measurement procedure. We demonstrate the deposition of spots with mean radii down to 34 nm and investigate the effect of the deposition time and the applied voltage on the spot size.

The setup for electrically assisted deposition is shown in Fig. 1. A FluidFM probe with a pyramidal-shaped tip is shown in the inset. The aperture at the apex is approximately 200 nm, and the spring constant of the cantilever is 2–3 N/m. The outside of the probe and the substrate were coated with fluorocarbon (FC)[10] to minimize wetting of the tip[6,11] and to create an hydrophobic insulating[9] layer on the substrate.

The proposed mechanism for the deposition is as follows: a voltage is applied between the liquid in the probe and the substrate, which causes electrostatic attraction between the two and the deformation of the meniscus at the aperture.[12] The flexible cantilever starts to bend downward. When the Maxwell stress exceeds the Laplace pressure, liquid will be extracted from the probe. The aqueous solution will make contact with the hydrophobic insulating layer. For the measured gap heights, we expect a constant stream of liquid to the substrate. We assume that possible discrete events occur on a much smaller time scale than the typical deposition times and call this a constant stream. The potential difference between the liquid and the substrate leads to electrowetting,[13] which causes the contact angle with the hydrophobic surface to decrease. The spreading of the liquid is fed by an

a)j.geerlings@utwente.nl.

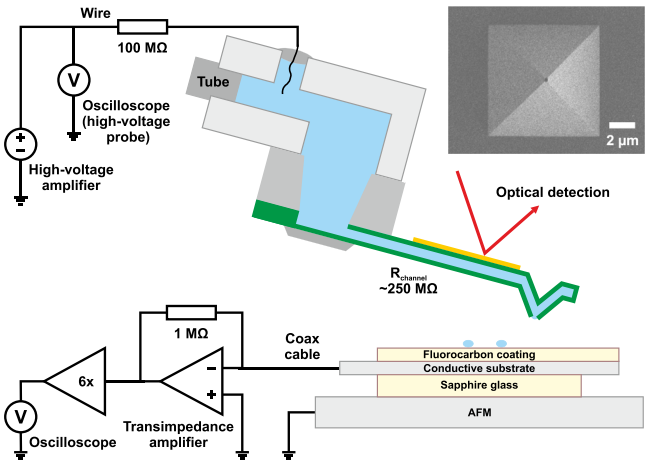

FIG. 1. Experimental setup with a pyramidal tip FluidFM probe. The inset shows a SEM image of the tip.

electrokinetic flow causing a stream of liquid with excess charge to the substrate. Depending on the dielectric strength of the insulator, the growing spot forms a capacitor with the underlying substrate or causes electric breakdown of the insulator. Both will reduce the electric force acting on the probe and the tip starts moving upward again. When a constant stream of liquid is assumed and a constant (advancing) contact angle, the droplet radius will show a third power relation with the spray time ($r \propto t^{1/3}$). After evaporation of the liquid, a dried deposit will remain on the substrate.

Deposition experiments were performed on a commercial (Bruker MultiMode) AFM. Probe holders with fluidic and electric connection were 3D printed to obtain a closed fluidic system similar to the FluidFM system.[8] The AFM was controlled by (Bruker) NanoScript, and a (Bruker NanoScope) signal access module (SAM) was inserted between the AFM and the controller to obtain the deflection signals. A waveform generator (Agilent 33220A) produced voltage pulses (in response to triggers from the SAM), which were subsequently amplified by a wideband amplifier (Krohn-Hite 7602M). Between the amplifier and a platinum wire in contact with the liquid, a 100 MΩ resistor was inserted to suppress electric breakdown of air between the tip and the substrate. The electric current was monitored by a transimpedance amplifier, which keeps the substrate at a virtual ground level. Vertical and lateral deflection signals from the AFM were recorded by an oscilloscope (Agilent DSO-X 3024A), along with the high-voltage pulses and the signals from the transimpedance amplifier.

The substrate consisted of a silicon chip with a layer of 2 nm titanium and 20 nm gold deposited by evaporation. To maximize the electric field near the tip for a given voltage, a thin hydrophobic layer of 20 ± 5 nm FC was used as insulator. This layer will break down around 1 V,[10] thereby allowing an easily detectable current signal during deposition and a constant tip voltage.

For the experiments, a mixture of deionized (DI) water, isopropyl alcohol (70 m%:30 m%), and sodium sulfate (33 mmol/l) with a conductivity of 2 mS/cm was used. The surface tension of this one-phase mixture[14] is expected to be of the order of 27 mJ/m^2.[15] For this solution, the measured contact angle on the substrate was of the order of 55° (advancing 57° and receding 28°). For DI water, the contact angle was greater than 90°. Based on the conductivity of 2 mS/cm, the channel resistance is about 250 MΩ.

Before each deposition experiment, a force distance curve was taken to relate the measured deflection voltage to the actual probe deflection. The average sensitivity was 27 ± 2 nm/V. The laser spot was focused on the base of the cantilever to maximize the detectable deflection range. During the experiments, the deposition behavior (for example, the spot sizes) changed. This can be attributed to the formation of salt crystals and the accumulation of other substances at the tip during the many hours of operation. To minimize this effect, the measurements presented in this letter were all taken within a stable time window of 2.5 h.

The experiments were performed in a dry N_2 environment with a relative humidity <5% at 22.0±0.9°C. Before each deposition experiment, the respective substrate area was scanned in contact mode at 200 µm/s with an estimated contact force of 200–400 nN. The obtained height profile was used to maintain a constant gap height between the tip and the substrate during lift mode. By applying voltage pulses, liquid could be deposited onto the substrate. Liquid deposition was not observed when the probe was brought in contact with the substrate (for the same pulse duration) without applying a voltage.

The effect of the height and duration of the voltage pulse on the spot size was studied by performing experiments with series of voltage pulses between 0.1 ms and 100 ms leading to an array of spots. After the deposition experiments, the substrate was scanned using a commercial AFM probe (Nanosensors PPP-NCHR) in tapping mode.

Minimal dried deposits with a mean diameter (averaged diameter in four directions) of 78 ± 12 nm were observed. In Fig. 2(a), a part of an array is shown as example. The smallest spot has a size of 68 nm and a height of 26.4 nm. This corresponds to a volume of 64 zeptoliter (assuming a half-spheroidal shape). In Fig. 2(b), the applied voltage pulse, deflection signal, and electric current for this particular spot are shown. The maximum deflection of the cantilever is 734 nm (initial gap height 940 nm), which indicates contactless deposition. At the end of the voltage pulse, oscillations with a frequency of 74.3 kHz can be observed. From the decay in amplitude, a Q-factor of 55 can be estimated. The resonance frequency and Q-factor of the dried out cantilever were 73.6 kHz and 158, respectively (obtained from thermal noise spectra measured by a Polytec MSA-400 Micro System Analyzer). It is therefore likely that the observed oscillation is simply the free oscillation of the cantilever. This indicates that the tip was not in contact with the deposited liquid when the 0.5 ms pulse ended. For longer pulse durations (>5 ms), the oscillation was mainly observed during the pulse with a frequency close to the resonance frequency. When the oscillation stopped (during the pulse), the liquid droplet is expected to have reached the tip.

In Fig. 3, voltage pulses of 100 ms were applied. The maximum deflection, maximum current (after the displacement currents subsided), and measured radius of the dried deposits are shown as function of the voltage for three different initial gap heights. For the 640 nm gap, the probe follows a normal deflection curve up to 55 V. Above this value,

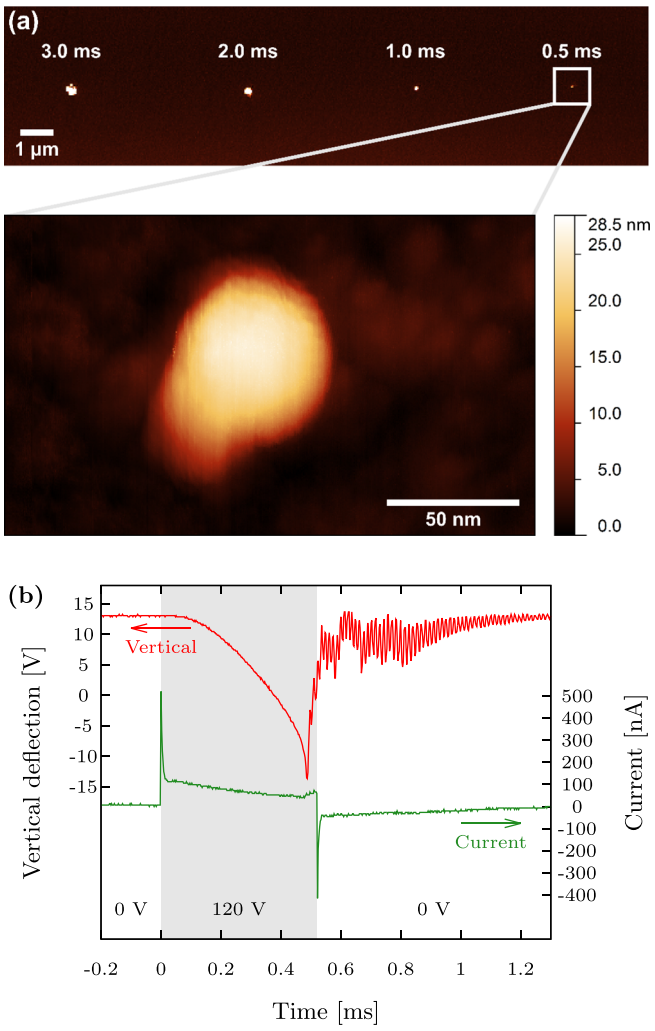

FIG. 2. (a) AFM scan of an array with dried deposits. The initial gap height before deposition was 940 nm. Deposits from pulses of 120 V during 3, 2, 1, and 0.5 ms are shown. The 0.5 ms dried deposit with an average diameter of 68 nm is shown in the detailed AFM scan. In (b), the voltage, deflection, and current signal for the 0.5 ms deposition are shown. The sensitivity of the vertical deflection was 27 nm/V, which gives a maximum deflection of 734 nm.

spraying occurs, which can be observed by the increase in current and the dried deposits afterwards. For the 940 nm gap, spraying started above 80 V, while for the 1940 nm gap no spraying was observed below 100 V. In most cases, the maximum deflection during deposition was smaller than the detector range (740 ± 32 nm) and the initial gap height. It should be noted that for the "highest points" in the 640 nm and 940 nm series pull-in and subsequent pull-off cannot be excluded. These blue and red points relate to the maximum deflection (first 2 ms in most cases). During most of the deposition phase, the deflection was well within range indicating contactless deposition.

In Fig. 4, the mean radius and the maximum height of the dried deposits are shown as function of the pulse duration for different voltages and initial gap heights. The measurements in Fig. 4(a) were performed with a resolution of 40 nm. The convolution of the tip shape with the dried deposits will a cause a slight overestimation of the spot radius.

Fig. 2(b) illustrates the deposition process more in detail. After the start of the voltage pulse, the probe moves downward. The gradual fall is most likely caused by the RC-

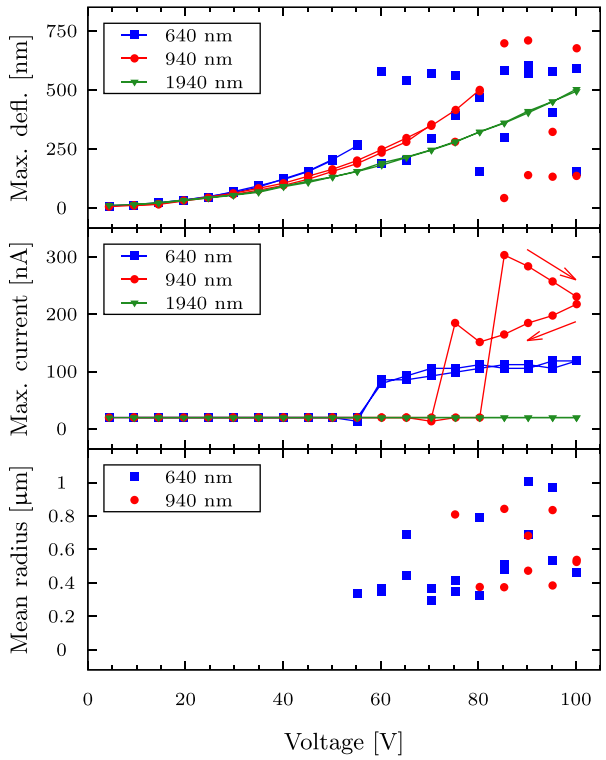

FIG. 3. Maximum deflection, maximum current (excluding displacement currents), and resulting dried deposits as function of the applied voltage. For three initial gap heights, the voltage was incremented up to 100 V and then decremented back to 5 V. Each 100 ms pulse was applied above a new location. Lines between the points are drawn as guide to the eye.

times in the system. At a certain point, spraying occurs and the probe moves upward again, because of the discharge of the probe-substrate capacitor.

When, in Fig. 3, the electrostatic deflection is taken into account, it shows that spraying occurs above an approximately similar average electric field for the 640 nm and 940 nm measurements ($E_{640\text{nm}} = \frac{55\,\text{V}}{(640-264)\,\text{nm}} = 146\,\text{MV/m}$ and $E_{940\text{nm}} = \frac{80\,\text{V}}{(940-500)\,\text{nm}} = 182\,\text{MV/m}$). For the 1940 nm gap, this electric field is not reached below 100 V ($E_{1940\text{nm}} = \frac{100\,\text{V}}{(1940-504)\,\text{nm}} = 70\,\text{MV/m}$) and spraying is indeed not observed. From the maximum currents (Fig. 3), we estimate the total resistance to be in the range of 0.2–1 GΩ, which indicates that the FC layer has completely broken down.

The measured dried deposits shown in Fig. 4 indicate that the spot size increases with time, up to at least 100 ms. Power law functions fitted to all the data points for the radius and height (with 95% confidence bounds) are given by $(0.17 \pm 0.03) \times t^{0.33 \pm 0.04}$ and $(107 \pm 41) \times t^{0.35 \pm 0.10}$, respectively. These time dependencies match extremely well with $t^{1/3}$, which indicates that a constant stream of liquid is present during deposition. The power law relation for the radius found here deviates from values reported for contact deposition methods such as NADIS[6] ($t^{0.26 \pm 0.04}$) and DPN[5] ($t^{0.5}$). According to the data in Figs. 3 and 4, there is no relation between spot size and voltage, but further work is required to confirm this.

In this letter, we presented an easily switchable nanoscale deposition technique for polar and ionic components. Liquid was deposited by the application of voltage pulses, whereas without the application of the voltage, no liquid was

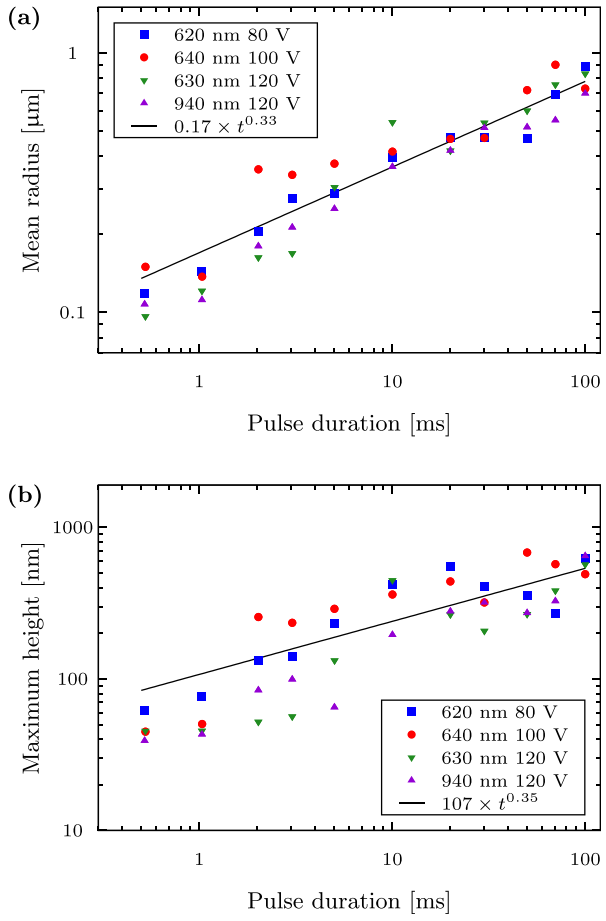

FIG. 4. Measured dried deposits as function of pulse duration. Each point represents the average of maximum three measurements. The black solid lines represent the best fits to a power function. (a) Mean radius (measurement resolution 40 nm) and (b) maximum height (measurement resolution <1 nm).

deposited. Spraying at 60 V, with an initial gap height of 640 nm, was observed by the electric current and the dried sodium sulfate deposits afterwards. The power laws found indicate that the volume of the deposits on the hydrophobic substrate increases linearly with the pulse duration. Minimal dried deposits of 78 ± 12 nm were obtained at a pulse duration of 0.5 ms, which is significantly smaller than results obtained with electrospray deposition from pulled capillaries[9] and comparable to the smallest results obtained with NADIS.[6] The non-contact nature of the technique presented in this letter allows for 3D nanodeposition and the study of forces involved in electrospray.

The authors would like to thank Professor J. G. E. Gardeniers for critical reading of the manuscript and SmartTip B.V. (The Netherlands) and Cytosurge AG (Switzerland) for providing the FluidFM probes. This work was carried out within the FunTips-project, funded by NWO/STW through a Vidi Grant (No. 10233).

[1]J. B. Fenn, M. Mann, C. K. Meng, S. F. Wong, and C. M. Whitehouse, Science **246**, 64 (1989).
[2]R. D. Piner, J. Zhu, F. Xu, S. Hong, and C. A. Mirkin, Science **283**, 661 (1999).
[3]A. Meister, S. Jerney, M. Liley, T. Akiyama, U. Staufer, N. F. de Rooij, and H. Heinzelmann, Microelectron. Eng. **67–68**, 644 (2003).
[4]B. L. Weeks, A. Noy, A. E. Miller, and J. J. De Yoreo, Phys. Rev. Lett. **88**, 255505 (2002).
[5]J. Jang, S. Hong, G. C. Schatz, and M. A. Ratner, J. Chem. Phys. **115**, 2721 (2001).
[6]L. Fabié and T. Ondarçuhu, Soft Matter **8**, 4995 (2012).
[7]S. Deladi, N. R. Tas, J. W. Berenschot, G. J. M. Krijnen, M. J. de Boer, J. H. de Boer, M. Peter, and M. C. Elwenspoek, Appl. Phys. Lett. **85**, 5361 (2004).
[8]A. Meister, M. Gabi, P. Behr, P. Studer, J. Vörös, P. Niedermann, J. Bitterli, J. Polesel-Maris, M. Liley, H. Heinzelmann, and T. Zambelli, Nano Lett. **9**, 2501 (2009).
[9]J.-U. Park, M. Hardy, S. J. Kang, K. Barton, K. Adair, D. K. Mukhopadhyay, C. Y. Lee, M. S. Strano, A. G. Alleyne, J. G. Georgiadis, P. M. Ferreira, and J. A. Rogers, Nat. Mater. **6**, 782 (2007).
[10]H. V. Jansen, J. G. E. Gardeniers, J. Elders, H. A. C. Tilmans, and M. Elwenspoek, Sens. Actuators A **41**, 136 (1994).
[11]J. Geerlings, E. Sarajlic, J. W. Berenschot, R. G. P. Sanders, L. Abelmann, and N. R. Tas, in *Proc. of the 27th IEEE Int. Conf. on MEMS, MEMS 2014* (Institute of Electrical and Electronics Engineers Inc., 2014), pp. 100–103.
[12]G. Taylor, Proc. R. Soc. A **280**, 383 (1964).
[13]F. Mugele and J.-C. Baret, J. Phys. Condens. Matter **17**, R705 (2005).
[14]D. K. Brenner, E. W. Anderson, S. Lynn, and J. M. Prausnitz, J. Chem. Eng. Data **37**, 419 (1992).
[15]G. Vázquez, E. Alvarez, and J. M. Navaza, J. Chem. Eng. Data **40**, 611 (1995).